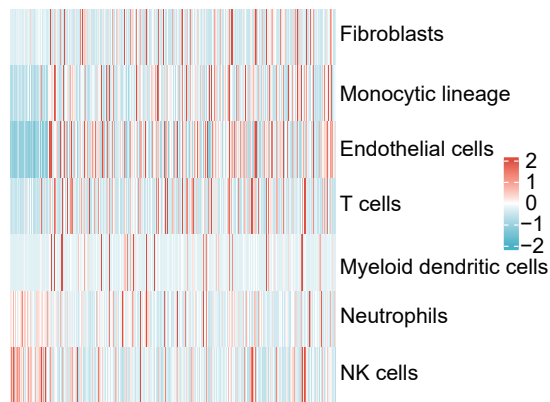
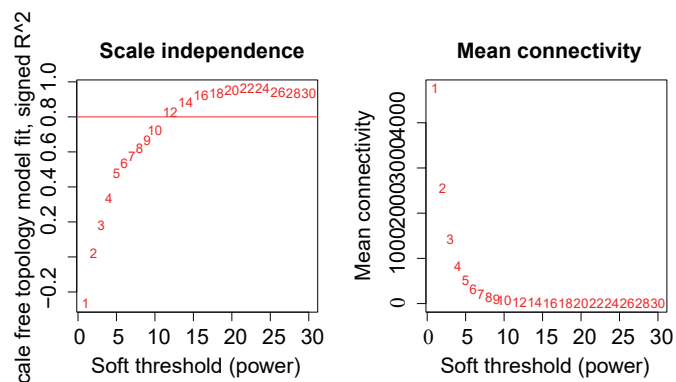
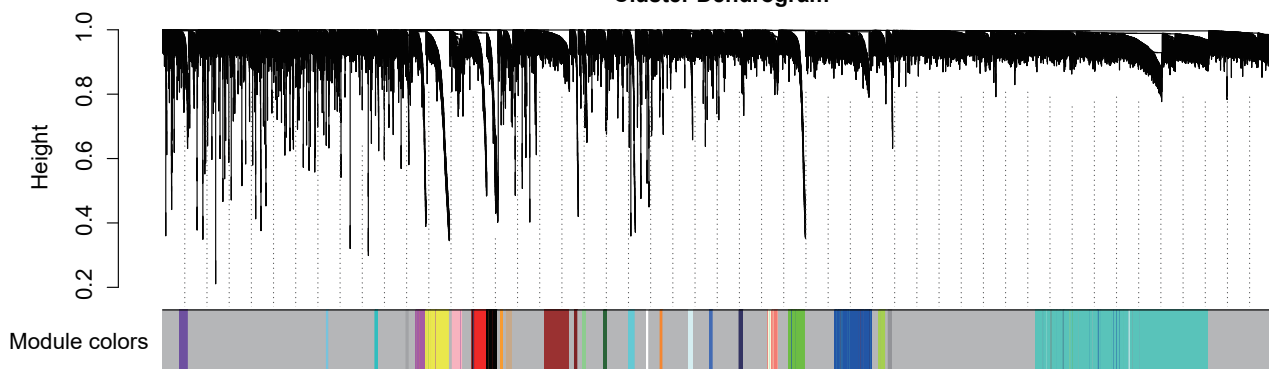
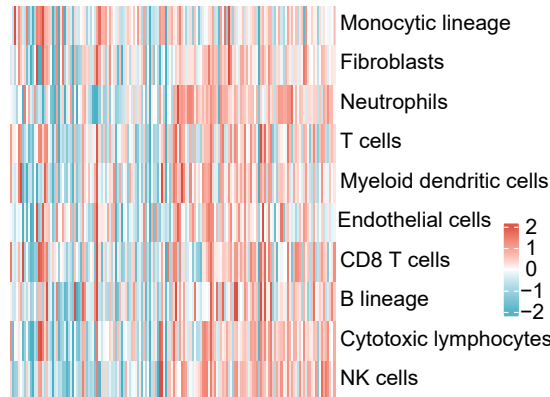
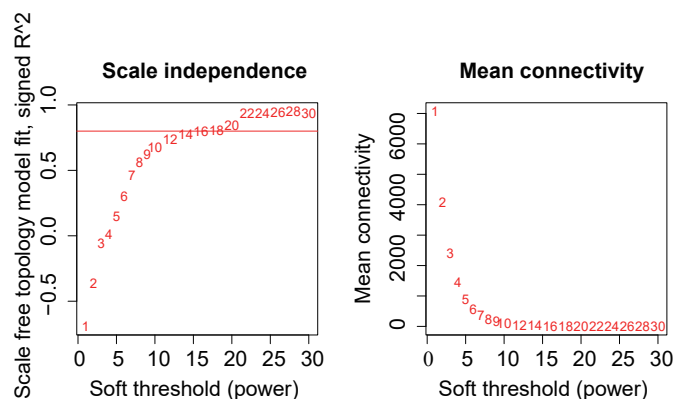
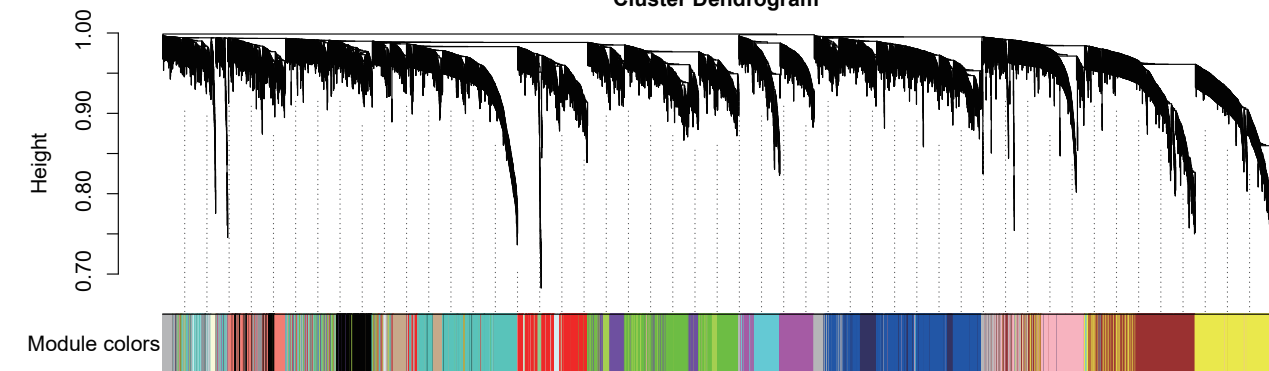
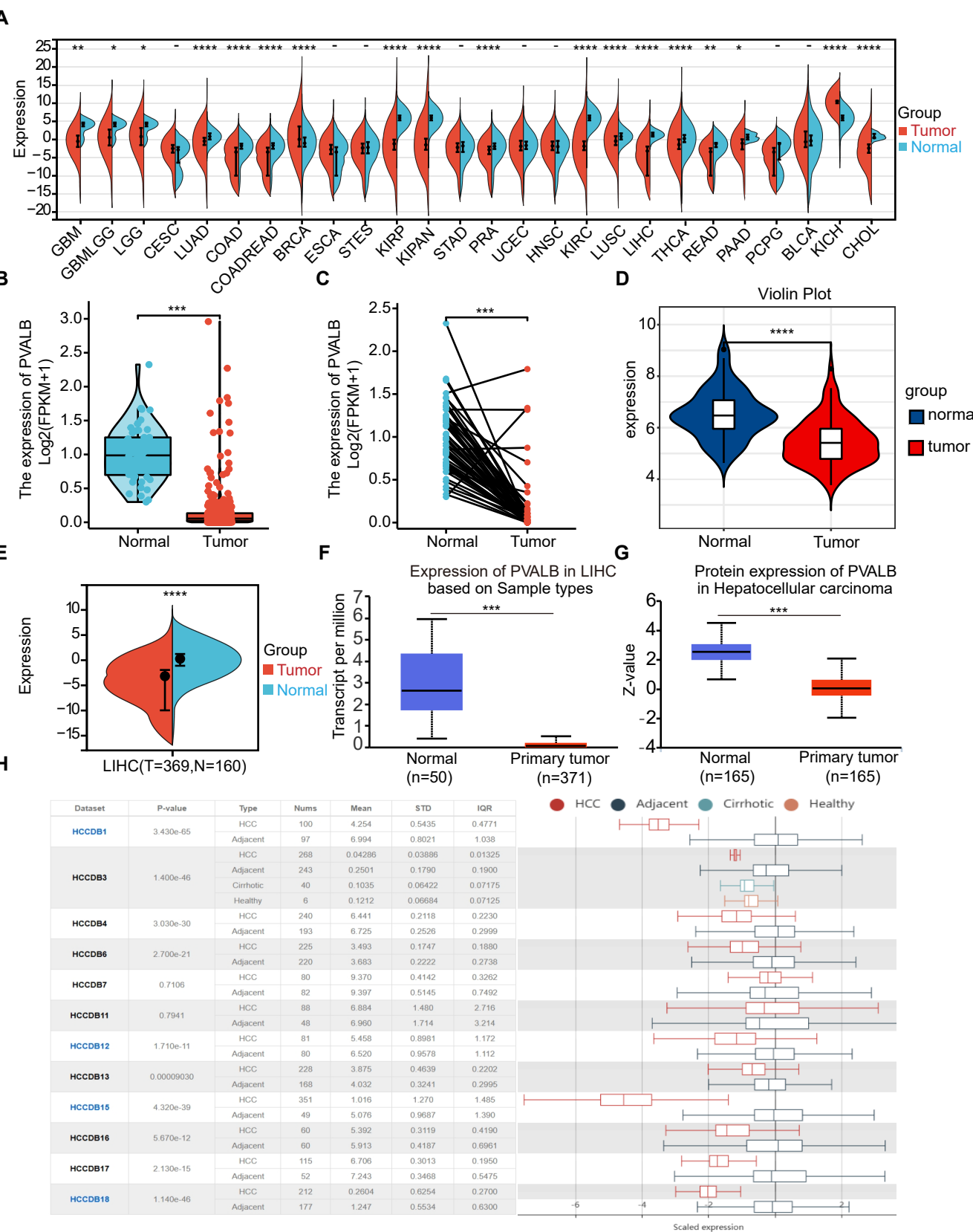
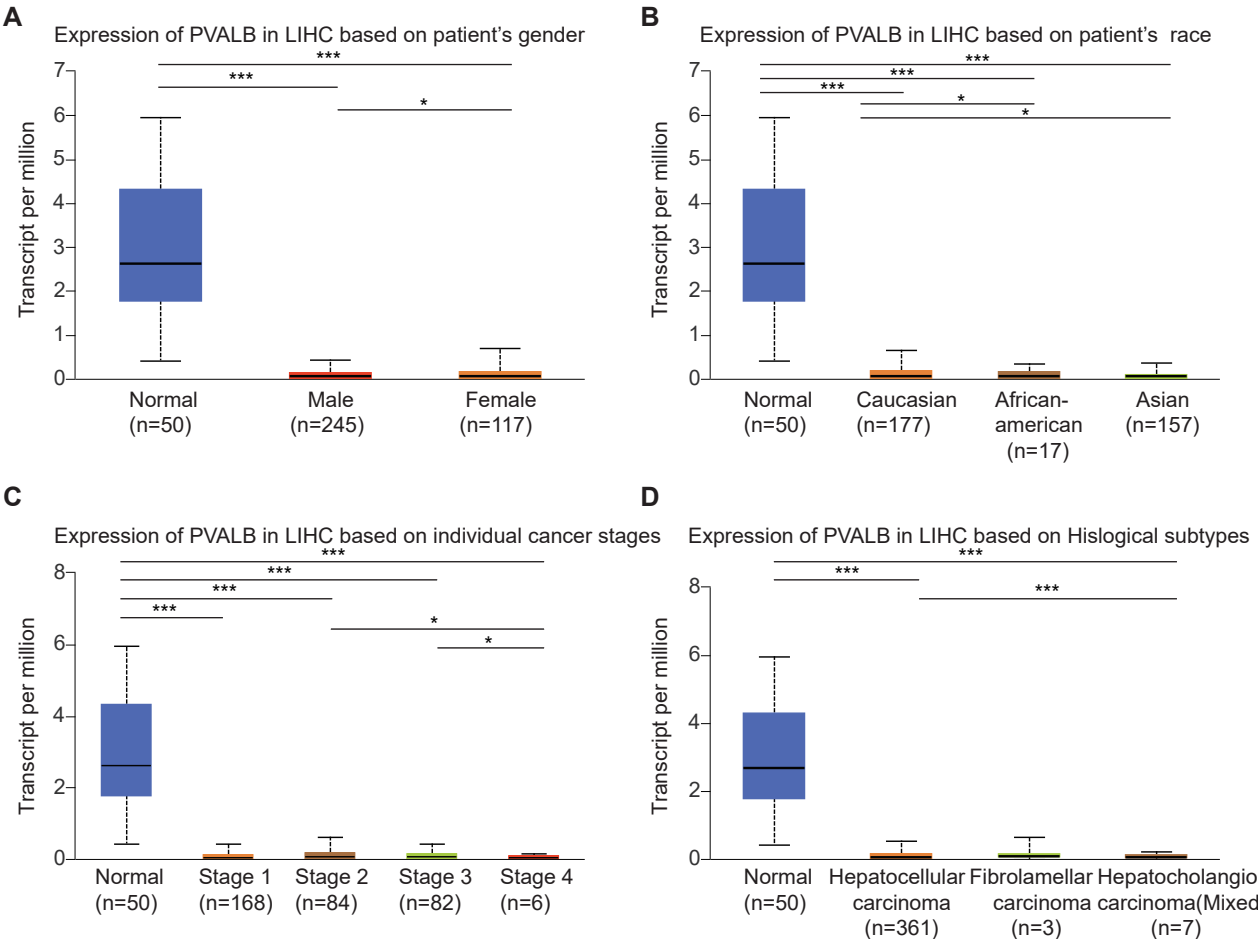


A**B****C****D****E****F**

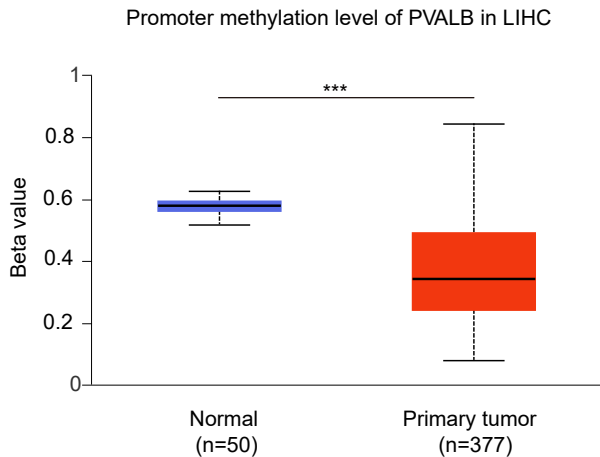
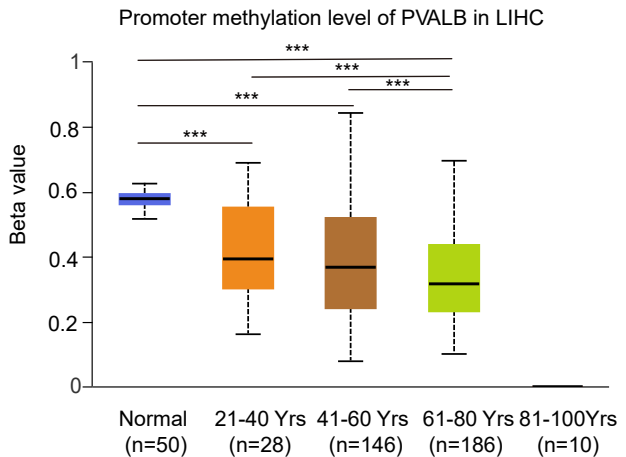
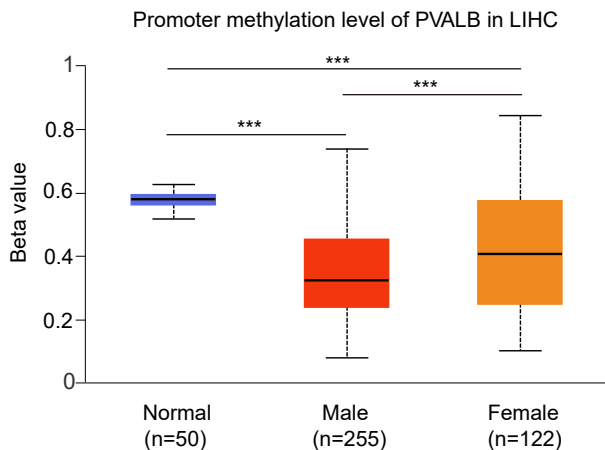
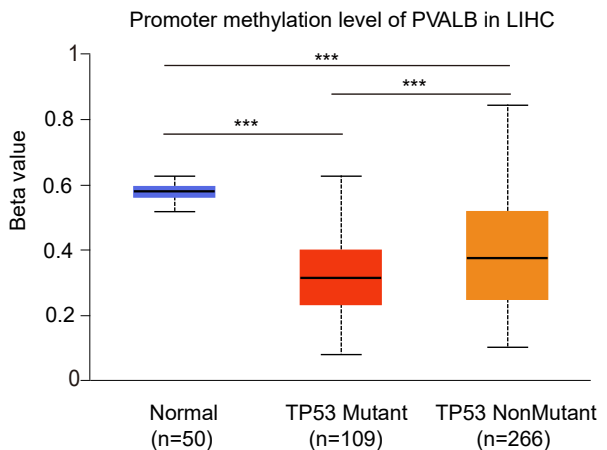
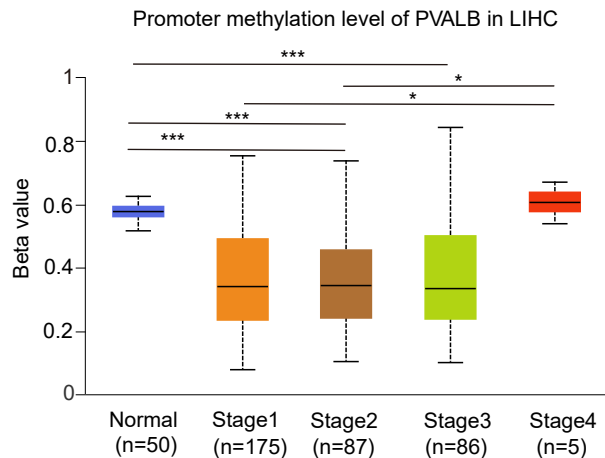
Supplementary Figure 1. Calculation of immune cell abundance and construction of weighted co-expression network. Heatmap illustrated the abundance of immune cell infiltration in (A) TCGA cohort. Determination of scale independence and average connectivity of (B) TCGA cohort in WGCNA. Dendrograms of all differentially expressed genes clustered in the (C) TCGA cohort. Heatmap illustrated the abundance of immune cell infiltration in (D) GSE54236 cohort. Determination of scale independence and average connectivity of (E) GSE54236 cohort in WGCNA. Dendrograms of all differentially expressed genes clustered in the (F) GSE54236 cohort.



Supplementary Figure 2. The expression of PVALB in HCC. (A) Differential expression of PVALB in tumor and normal tissue across distinct cancers. (B-C) Expression level of PVALB in HCC tissue and normal tissue based on TCGA database. Expression level of PVALB in HCC were lower than normal tissue by (D) GSE54236 dataset and (E) TCGA +GTEX databases. The (F) mRNA and (G) protein expression level of PVALB in HCC tissue and normal tissue by UALCAN online website. (H) Comparison of PVALB expression level in HCC tissue and adjacent tissue in 12 cohorts of HCCDB, of which 10 cohorts were significant.(****p < 0.0001, ***p < 0.001, **p < 0.01, *p < 0.05)

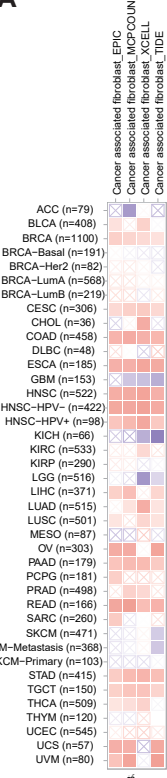


Supplementary Figure 3. Correlation of PVALB expression with clinicopathologic features in HCC patients based on the UALCAN online site. (A) gender; (B) race; (C) cancer stages. (D) histologic subtypes.(*p < 0.001, *p < 0.05)**

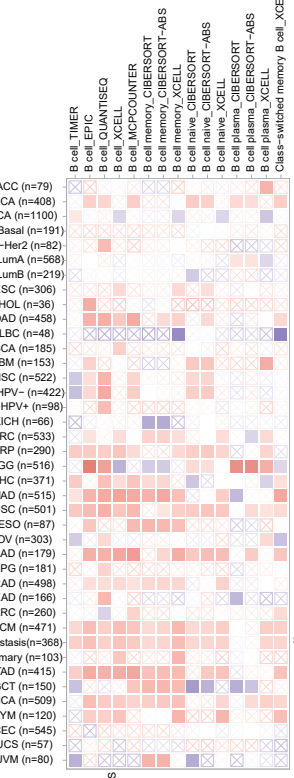
A**B****C****D****E**

Supplementary Figure 4. PVALB promoter methylation level were associated with clinicopathological features. (A) Sample type (B) Patient age (C) Patient gender (D) TP53 mutation status (E) Cancer stage.(*p < 0.001, *p < 0.05)**

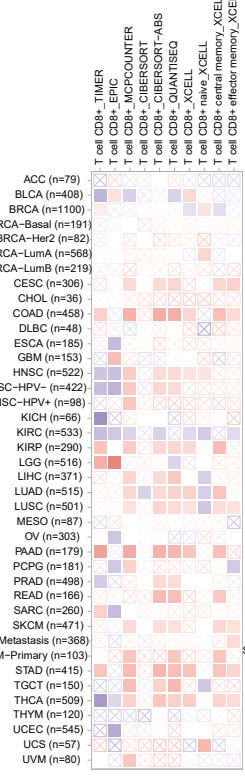
A



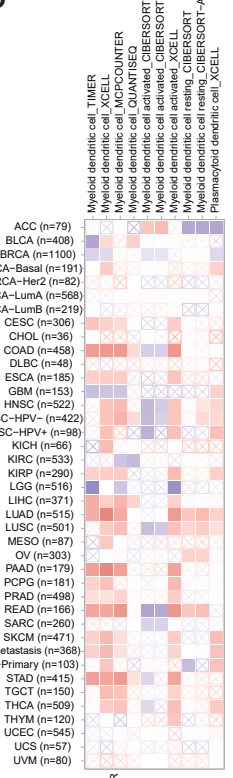
B



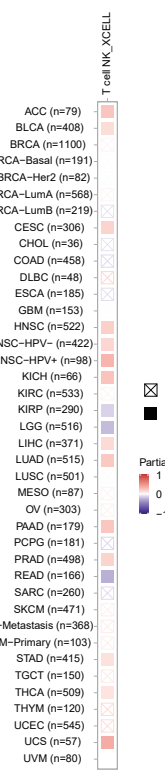
C



D



E



F

G

H

I

J

Legend:

■ p > 0.05
■ p ≤ 0.05
■ Partial_Cor
1
0
-1

F

■ p > 0.05
■ p ≤ 0.05
■ Partial_Cor
1
0
-1

G

■ p > 0.05
■ p ≤ 0.05
■ Partial_Cor
1
0
-1

H

■ p > 0.05
■ p ≤ 0.05
■ Partial_Cor
1
0
-1

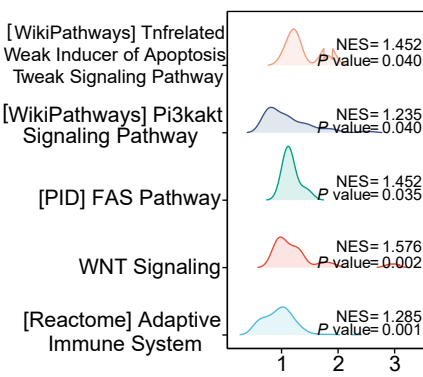
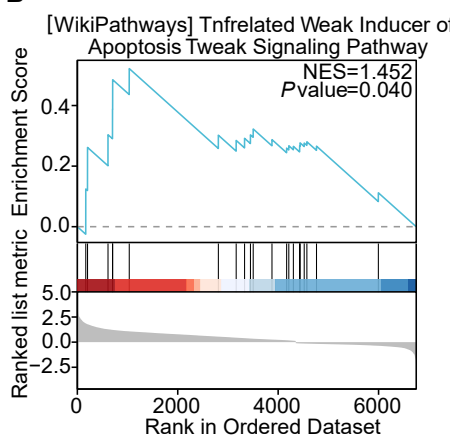
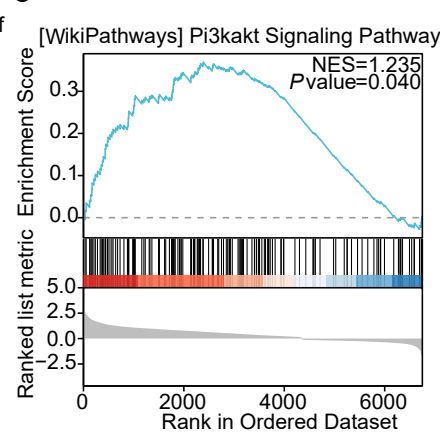
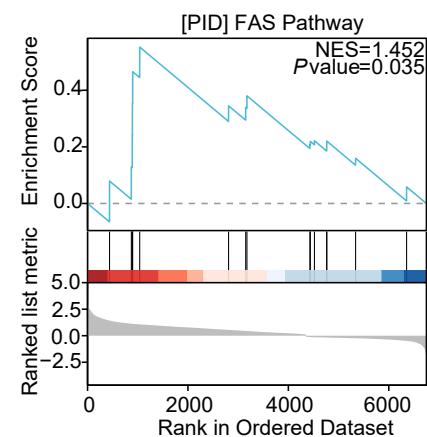
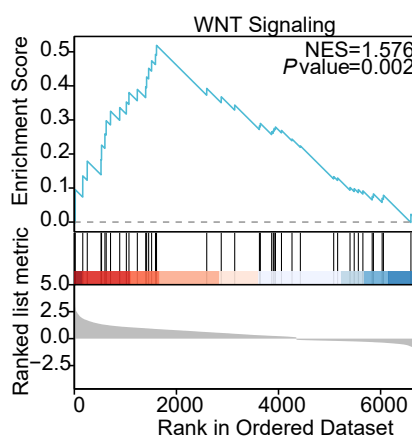
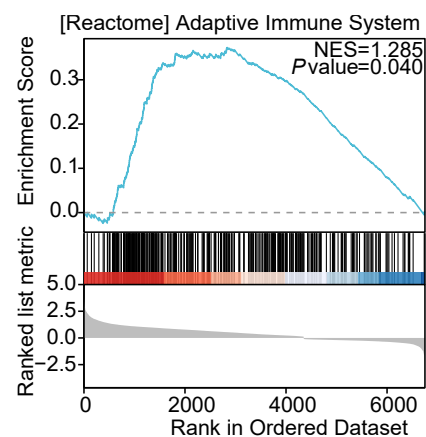
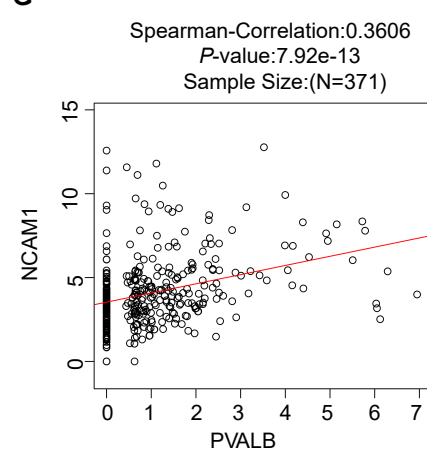
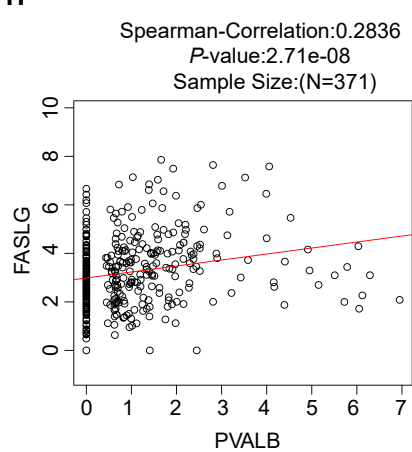
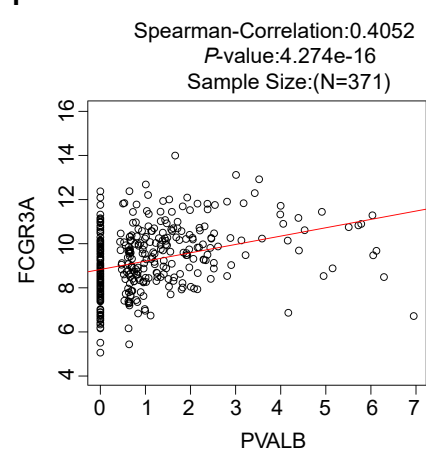
I

■ p > 0.05
■ p ≤ 0.05
■ Partial_Cor
1
0
-1

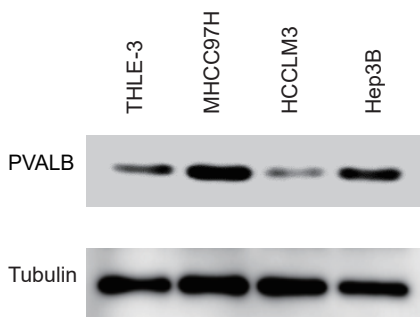
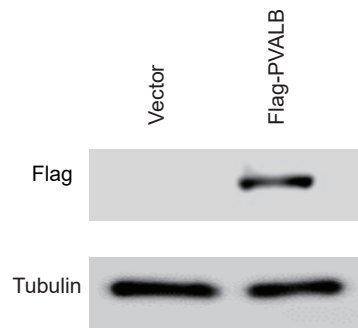
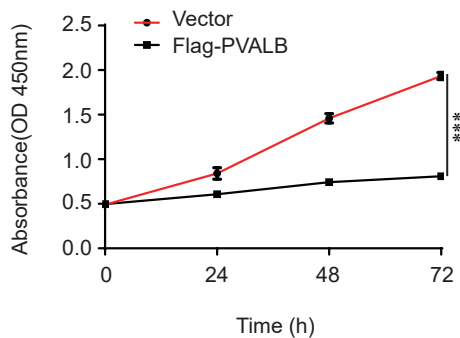
J

■ p > 0.05
■ p ≤ 0.05
■ Partial_Cor
1
0
-1

Supplementary Figure 5. Correlation between PVALB and immune infiltration in pan- cancer obtained based on different algorithms (A) Cancer associated fibroblast (B) B cell (C) T cell CD8+ (D) Myeloid dendritic cell (E) T cell NK (F) T cell regulatory (G) T cell follicular helper (H) Monocyte (I) Macrophage (J) NK cell.

A**B****C****D****E****F****G****H****I**

Supplementary Figure 6. PVALB and Fas/FasL signaling pathway. (A) Mountain range plot showed the five pathways enriched for PVALB. GSEA results showed differential enrichment of genes with high PVALB expression (B) Tnfrelated Weak Inducer of Apoptosis Tweak Signaling Pathway; (C) Pi3kakt Signaling Pathway; (D) Fas Pathway; (E) WNT Pathway; (F) Adaptive Immune System. NES, normalized enrichment score; $P < 0.05$. (G-I) Scatter plots showed correlation between FCGR3A (CD16), NCAM1 (CD56), FASLG (FasL) and PVALB in HCC.

A**B****C**

Supplementary Figure 7. Selection and validation of cell lines and CCK8 assay. (A) Expression of PVALB in different cell lines **(B)** The validation of the transfection efficiency of the PVALB gene before doing the phenotypic function experiment**(C)** CCK8. (**p < 0.001)